Gazi Üniversitesi
Fen Bilimleri Dergisi
PART C: TASARIM VE TEKNOLOJİ

Gazi University
Journal of Science
PART C: DESIGN AND TECHNOLOGY

GU J Sci, Part C, 11(2): 464-474 (2023)

The Implementation of Internal Mode Control Method to SEPIC Converter for Battery Charging Systems

Fatih Süleyman TAŞKINCAN[1*] Ahmet KARAARSLAN[1] Zafer ORTATEPE[2]

[1] *Ankara Yıldırım Beyazıt University, Faculty of Engineering and Naturel Science, The Department of Electrical and Electronics Engineering, Ankara, Turkey*

[2]*Pamukkale University, Faculty of Technology, The Department of Automotive Engineering, Denizli, Turkey*

Article Info:

Research article
Received: 24/09/2022
Revision: 04/11/2022
Accepted: 01/03/2023

Keywords

Internal mode control
Battery charging system
SEPIC converter

Makale Bilgisi

Araştırma makalesi
Başvuru:24/09/2022
Düzeltme: 04/11/2022
Kabul: 01/03/2023

Anahtar Kelimeler

Dahili mod kontrolü
Batarya şarj sistemi
SEPIC dönüştürücü

Graphical/Tabular Abstract (Grafik Özet)

In this paper, internal model control (IMC) method, which is model based approach offers more robust and better reference tracking capability than conventional controllers for the unstable process, is applied to SEPIC topology used in battery charging system for military implementations. / Bu çalışmada, askeri uygulamalar için batarya şarj sistemlerinde kullanılan SEPIC topolojisine, kararsız süreçler için geleneksel denetleyicilere göre daha sağlam ve daha iyi referans izleme yeteneği sunan model tabanlı bir yaklaşım olan dahili mod kontrol (IMC) yöntemi uygulanmıştır.

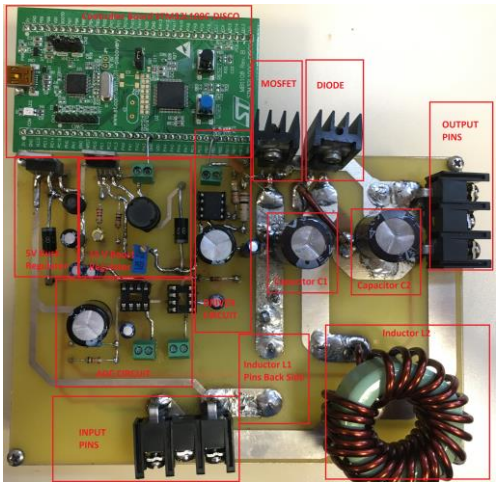

***Figure A**: The laboratory setup of the SEPIC board /**Şekil A:**. SEPIC bordunun laboratuvar kurulumu*

Highlights (Önemli noktalar)

- *IMC method, which is model based approach offers more robust and better reference tracking capability. / Model tabanlı bir yaklaşım olan IMC yöntemi, daha sağlam ve daha iyi referans izleme yeteneği sunar.*

***Aim (Amaç):** When a system is not based on a model, it is possible to encounter some problems in the control of the system, such as dead time and non-linearity. This study provides better performance of the system by using model based control approach. / Bir sistem bir modele dayalı olmadığında, sistemin kontrolünde ölü zaman ve doğrusal olmama gibi bazı sorunlarla karşılaşmak mümkündür. Bu çalışma, model tabanlı kontrol yaklaşımı kullanarak sistemin daha iyi performans göstermesini sağlar.*

***Orginality (Özgünlük):** IMC method implemented SEPIC converter is show better setpoint monitoring and more robustness for unstable process compared to conventional methods. / IMC yöntemi uygulanan SEPIC dönüştürücü, geleneksel yöntemlere kıyasla kararsız süreçler için daha iyi ayar noktası izleme ve daha sağlamlık gösterir.*

***Results (Bulgular):** Simulation and experimental outcomes reveale controller's robustness in both transient and steady-state conditions, when compared to the conventional PI method. / Simülasyon ve deneysel sonuçlar, geleneksel PI yöntemiyle karşılaştırıldığında hem geçici hem de kararlı durum koşullarında denetleyicinin sağlamlığını ortaya koymaktadır.*

***Conclusion (Sonuç):** IMC can be regarded as a suitable control method for conventional power supplies that provide quick response and steady-state benefits. / IMC, hızlı yanıt ve kararlı durum faydaları sağlayan geleneksel güç kaynakları için uygun bir kontrol yöntemi olarak kabul edilebilir.*

*Corresponding author, karaarslantemh@gmail.com
DOI: 10.29109/gujsc.1179763

GU J Sci, Part C, 11(2): 464-474 (2023)

Gazi Üniversitesi
Fen Bilimleri Dergisi
PART C: TASARIM VE TEKNOLOJİ

Gazi University
Journal of Science
PART C: DESIGN AND TECHNOLOGY

http://dergipark.gov.tr/gujsc

The Implementation of Internal Mode Control Method to SEPIC Converter for Battery Charging Systems

Fatih Süleyman TAŞKINCAN[1*] Ahmet KARAARSLAN[1] Zafer ORTATEPE[2]

[1] *Ankara Yıldırım Beyazıt University, Faculty of Engineering and Naturel Science, The Department of Electrical and Electronics Engineering, Ankara, Turkey*

[2]*Pamukkale University, Faculty of Technology, The Department of Automotive Engineering, Denizli, Turkey*

Article Info

Research article
Received:24/09/2022
Revision: 04/11/2022
Accepted: 01/03/2023

Keywords

Internal mode control
Battery charging system
SEPIC converter

Abstract

In this paper, internal model control (IMC) method, which is model based approach that offers more robust and better reference tracking capability than conventional controllers for the unstable process, is applied to SEPIC topology used in battery charging system for military implementations. When a system is not based on a plant model, it is possible to encounter some problems such as dead time and non-linearity in controlling of the system. The purpose of the SEPIC topology is to eliminate the disadvantage of other converter types such as buck/boost and cúk converters that are used for similar applications in reversing the output voltage. In addition, a great amount of voltage and current stress on a component causes the power board to overheat in such converters and requires additional cooling equipment. These problems are not encountered in SEPIC topology. Also, this topology provides high efficiency, step-up/step-down voltage conversion, and excellent transient state response over a wide range. The performance of IMC method applied on SEPIC converter is detailed analyzed in terms of simulation studies that are obtained by using MATLAB/Simulink and experimental studies.

Akü Şarj Sistemleri İçin Dahili Mod Kontrol Yönteminin SEPIC Dönüştürücüye Uygulanması

Makale Bilgisi

Araştırma makalesi
Başvuru:24/09/2022
Düzeltme: 04/11/2022
Kabul: 01/03/2023

Anahtar Kelimeler

Dahili mod kontrolü
Batarya şarj sistemi
SEPIC dönüştürücü

Öz

Bu çalışmada, askeri uygulamalar için batarya şarj sistemlerinde kullanılan SEPIC topolojisine, kararsız süreçler için geleneksel denetleyicilere göre daha sağlam ve daha iyi referans izleme yeteneği sunan model tabanlı bir yaklaşım olan dahili mod kontrol (IMC) yöntemi uygulanmıştır. Bir sistem, bir modele dayalı olmadığında, sistemin kontrolünde ölü zaman ve doğrusal olmama gibi bazı sorunlarla karşılaşmak mümkündür. SEPIC topolojisinin amacı, benzer uygulamalar için kullanılan buck/boost ve cúk dönüştürücüler gibi diğer dönüştürücü türlerinin çıkış geriliminin ters çevrilmesindeki dezavantajını ortadan kaldırmaktır. Ayrıca, bir bileşen üzerindeki büyük miktarda voltaj ve akım stresi, bu tür dönüştürücülerde güç kartının aşırı ısınmasına neden olur ve ek soğutma ekipmanı gerektirir. SEPIC topolojisinde bu problemlerle karşılaşılmaz. Ayrıca, bu topoloji, geniş bir aralıkta yüksek verimlilik, yükseltme/düşürme gerilim dönüşümü ve mükemmel geçici durum yanıtı sağlar. SEPIC dönüştürücü üzerinde uygulanan IMC yönteminin performansı, MATLAB/Simulink kullanılarak elde edilen simülasyon çalışmaları ve deneysel çalışmalar açısından detaylı olarak incelenmiştir.

1. INTRODUCTION (GİRİŞ)

DC-DC power converters are required to respond dynamically to sudden variations in frequency, load and input voltage. In addition, they must provide reliable and efficient output voltage without voltage sag and swell. Due to the heat, the efficiency of linear regulators (LRs) is lower than switching mode power supplies (SMPS) though they produce small ripples of output voltage. On the contrary, the LRs do not have a step-up capability, they are only step-down the voltage. Therefore, they are preferred in low power applications. The SMPS is used in all power applications due to high efficiency, lower

*Corresponding author, e-mail: karaarslantemh@gmail.com
DOI:10.29109/gujsc.1179763

switching loss and the most important one is reliability.

SMPS stores energy using various energy storage components such as capacitor and inductor. The energy that is stored in these components can be transferred to the output using different control methods through switching elements. One of the popular methods for controlling turn-on and turn-off mode of a switching device to transfer energy to load side is Pulse Width Modulation (PWM) that involves adjusting the width of a high-frequency pulse signal. Different SMPS topologies are available to be used by power electronics societies for various purposes. Boost/buck/buck-boost converters, most widely used topologies, are called non-isolated topologies because the lack of galvanic isolation between input/output voltages.

The Cúk and SEPIC topologies have been improved by adding low-pass filter to conventional topologies [1]. Output voltage ripple for this type of converter is reasonable and can be less than 2% [2]. Since there are two inductors in these topologies, it is called a two-stage converter, and both input and output currents are naturally filtered with an LC low pass filter. Also, charging and discharging capacitors by means of inductors prevents high current increases and thistable 2 makes the topology efficient [3]. Compared to Cúk converter, SEPIC converter has an advantage in that it produces an output voltage with rectified polarity.

In [4] and [5], Garcia de Viculia et al. analyzed the SEPIC converter in discontinuous conduction mode (DCM) and continuous conduction mode (CCM). In [6], transfer function of the SEPIC converter is calculated by state space averaging (SSA) method that is operated in CCM using feedback control design. In [7], R. Jose et al. have compared various SEPIC converter topologies. They have obtained the new resonant SEPIC converter with higher efficiency, smaller size and better transient response.

There are situations where switching converter such as SEPIC topology may need to function as a power supply, as well as maintain batteries that are used in military applications. The SEPIC converter that is designed properly can supply several amps continuously if the load demands it. The control methods used can directly impact the output voltage of the SMPS, making the performance of these algorithms a crucial factor to consider. Due to its effectiveness and straightforwardness in linear systems, the Proportional-Integral-Derivative (PID) control method is commonly favored in SMPS topologies. There are also some problems such as non-linearity and dead time in controlling the dynamic plant of the model in the PID control method [8]. The development of model-based control (MBC) approaches has been propelled by these concerns. Compared to the conventional ones, the Internal Mode Control (IMC) method, which is one of the MBC methods, shows a better reference tracking capability and more robustness for unbalanced applications [9]. The IMC method estimates the plant output in parallel and according to the estimation, applies a corrective effect [10]. In addition, the stability of IMC method depends on the plant and the controller such as the conventional control methods [11].

A new technique for obtaining a parallel model to the plant is presented in reference [9], a single-input single-output (SISO) system was then utilized by Garcia and Morari [10]. This approach incorporates various conventional techniques such as the dead-beat controller, Dahlin method and Smith estimator. Afterwards, this approach is integrated into discrete-time multiple-input multiple-output (MIMO) systems [12]. Reference [13] presents a boost-type DC-DC converter operating in CCM utilizes a two degrees of freedom (2DOF) IMC design to regulate the output voltage. Xiaodong Sun et al. analyzed a bearingless permanent magnet synchronous motor (BPMSM) by using IMC and inverse system technique in [14]. In [15], a new controller is designed for permanent magnet synchronous motor (PMSM) using both support vector machine generalized inverse (SVMGI) and IMC.

In this paper, IMC method is implemented for a SEPIC converter for battery charging system used in military applications due to the better setpoint monitoring and more robustness for unstable process compared to conventional methods. The theory and principle of SEPIC converter are given in part 2. Control strategies of the IMC and its comparison with the conventional PI control method is described for the SEPIC converter in part 3. The design of the topology is given in part 4. Simulation and test bench results are presented in part 5 and 6, respectively. Conclusion part is also given in the last chapter.

2. THEORY AND PRINCIPLES OF SEPIC CONVERTER (SEPIC DÖNÜŞTÜRÜCÜNÜN TEORİSİ VE PRENSİPLERİ)

2.1. The Operation of SEPIC Converter (SEPIC Dönüştürücünün Çalışması)

The fact that it has a non-inverting structure has made the use of SEPIC converter popular. The SEPIC converter can maintain a stable output voltage despite variations in the input voltage,

moreover, it is possible for the output voltage to be higher or lower than the input voltage. Applied duty cycle of the switching device can be modified to achieve desired output voltage or source current. It is a fourth-order time-varying converter with two switching states, one MOSFET, one diode, two inductors and two capacitors. The topology diagram of a typical SEPIC converter is illustrated in Figure 1.

The input side of SEPIC converter consists of an inductor (L_1) and switching element (S), like the standard boost converter, from which an output voltage higher than the input voltage can be obtained. When the switching element S is turned-on, the inductor L_1 is charged by current V_{in}/L_1. Besides, due to the diode D has reverse biased, no current flows through it and therefore inductor L_2 is charged by current V_{C1}/L_2.

When the switching element S is turned-off, currents i_{L1} and i_{L2} flow to the load through diode D. Thus, the capacitor C_1 charges through the inductor L_1; Capacitor C_2 charges through inductors L_1 and L_2. The voltage across the inductor L_2 equals to $-V_o$ during the turn-off state. In this mode, energy flows from inductors L_1 and L_2 to the load. Modulation Index (MI) that is related to duty cycle, input and output voltage is similar with Cûk converter without reverse polarity.

$$MI = V_o/V_{in} = D/(1-D) \quad (1)$$

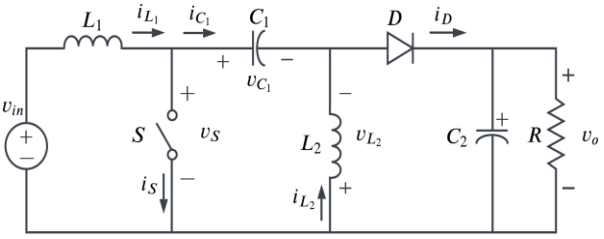

Figure 1. The structure of SEPIC Converter

2.2. State Space Modelling Of SEPIC Converter

(SEPIC Dönüştürücünün Durum Uzay Modeli)

The general state space equations are given in (2) and (3), respectively.

$$\dot{x} = Ax + B \quad (2)$$

$$y = Cx + Du \quad (3)$$

Where, x represents state-space vector, $\dot{x}$ represents state variable vector; u represents input signal; y represents output signal; A represents state matrix; B represents vector; C represents vector associated with the state variable and D represents vector relating input to the output. Also, both turn-on and turn-off modes are given in Figure 2 by using CCM operation.

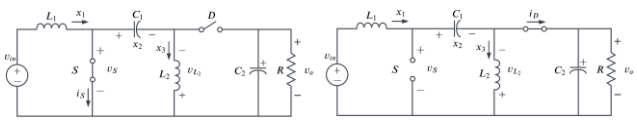

(a) (b)

Figure 2. Operating modes of SEPIC converter (a) the switch is turn-on state, (b) the switch is turn-off state

The state variables are considered as $x_1 = i_{L_1}$, $x_2 = v_{C_1}$, $x_3 = i_{L_2}$ and $x_4 = v_{C_2}$. In Figure 2 (a), when switch is turn-on, SEPIC converter state space model is expressed (4) and (5).

$$V_{out} = [0 \quad 0 \quad 0 \quad 1]\begin{bmatrix} x_1 \\ x_2 \\ x_3 \\ x_4 \end{bmatrix} \quad (5)$$

In Figure 2 (b), when switching element is turn-off, SEPIC converter state space variables are expressed given (6) and (7).

$$V_{out} = [0 \quad 0 \quad 0 \quad 1]\begin{bmatrix} x_1 \\ x_2 \\ x_3 \\ x_4 \end{bmatrix} \quad (7)$$

During the model extraction, switching element is assumed ideal and the parasitic elements ($r_{L1}, r_{L2}, r_{C1}, r_{C2}$) are assumed to be negligible, state space model is expressed as:

$$\dot{x} = [A_1 d + A_2 d^-]x + [B_1 d + B_2 d^-]u \quad (8)$$

$$y = [C_1 d + C_2 d^-]x + [D_1 d + D_2 d^-]u \quad (9)$$

where $d = \frac{t_{on}}{T}$ and $d^- = 1 - d = \frac{t_{off}}{T}$. DC and AC parts of the variables d, x, u and y can be expressed given below:

$$\begin{bmatrix} \dot{x_1} \\ \dot{x_2} \\ \dot{x_3} \\ \dot{x_4} \end{bmatrix} = \begin{bmatrix} 0 & 0 & 0 & 0 \\ 0 & 0 & 1/C_1 & 0 \\ 0 & -1/L_2 & 0 & 0 \\ 0 & 0 & 0 & -1/RC_2 \end{bmatrix}\begin{bmatrix} x_1 \\ x_2 \\ x_3 \\ x_4 \end{bmatrix} + \begin{bmatrix} 1/L_1 \\ 0 \\ 0 \\ 0 \end{bmatrix} V_{in} \quad (4)$$

$$\begin{bmatrix} \dot{x_1} \\ \dot{x_2} \\ \dot{x_3} \\ \dot{x_4} \end{bmatrix} = \begin{bmatrix} 0 & -1/L_1 & 0 & -1/L_1 \\ 1/C_1 & 0 & 0 & 0 \\ 0 & 0 & 0 & -1/L_2 \\ 1/C_2 & 0 & -1/C_2 & -1/RC_2 \end{bmatrix}\begin{bmatrix} x_1 \\ x_2 \\ x_3 \\ x_4 \end{bmatrix} + \begin{bmatrix} 1/L_1 \\ 0 \\ 0 \\ 0 \end{bmatrix} V_{in} \quad (6)$$

$$\begin{aligned} d &= D + \tilde{\delta} \\ x &= X + \tilde{x} \\ u &= V_{in} + \tilde{v}_{in} \\ y &= V_{out} + \tilde{v}_{out} \end{aligned} \quad (10)$$

The first terms in the equations represent the DC signal part, and the second terms represent the AC signal part. When these equations are put into a time-weighted average equation, they can be expressed as (11) and (12).

To determine a signal response, AC signal disturbances at the input ($\tilde{v}_{in}$) are neglected as (13) and (14). To solve the equation, it needs to be transformed to the frequency domain given (15). The relationship between control and output can be calculated as (16).

3. THEORY AND PRINCIPLES OF IMC METHOD (IMC Metodunun Teorisi ve Prensipleri)

The conventional feedback model and a specific property of the proposed IMC method that implemented to the SEPIC converter is given in Figure 3 (a) and (b), respectively.

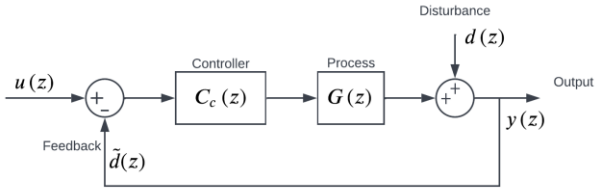

(a)

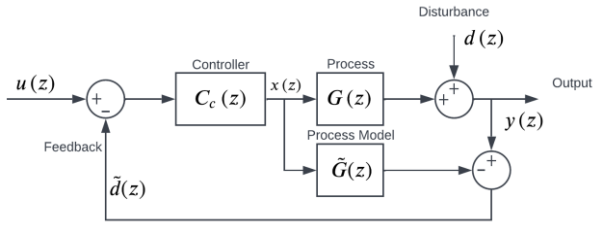

(b)

Figure 3. (a) Conventional feedback structure of the system (b) proposed IMC method of the System

Figure 3 (b) shows that the plant model $\tilde{G}(z)$ is positioned in parallel with G(z), which enables it to make predictions. When the plant model $\tilde{G}(z)$ is equivalent to the plant G(z), any disturbance in the plant is solely caused by the disturbance d(z).

According to the Figure 3 (b), the transfer functions of $m(z)$ and $y(z)$ for the IMC method are calculated as follows:

$$x(z) = \frac{G_c(z)}{1+G_c(z)(\,G(z)-\tilde{G}(z))}(u(z) - \tilde{d}(z) \quad (17)$$

$$y(z) = d(z) + \frac{G_c(z)G(z)}{1+G_c(z)(\,G(z)-\tilde{G}(z))}\big(u(z) - \tilde{d}(z)\big) \quad (18)$$

For stability, the roots of the characteristic functions given below should be in the unit cycle.

$$\frac{1}{G_c(z)} + \big(\,G(z) - \tilde{G}(z)\big) = 0 \quad (19)$$

$$\frac{1}{G(z)\,G_c(z)} + \frac{1}{G_c(z)}\big(\,G(z) - \tilde{G}(z)\big) = 0 \quad (20)$$

The benefits of the IMC are analyzed given below:

Stability: The model is assumed ideal; and the plant model $\tilde{G}(z)$ is identical to $G(z)$. Characteristic functions are transformed below equations, specifying that the poles are into the unit loop.

$$\frac{1}{G_c(z)} = 0 \; and \; \frac{1}{G(z)\,G_c(z)} = 0 \quad (21)$$

Control: If system control cannot be performed, it is important how close the controller should be to the ideal control point. An inverse model provided below is utilized to represent the plant as invertible and non-invertible components during the control design process:

$$\tilde{G}(z) \; = \tilde{G}_+(z)\,\tilde{G}_-(z) \quad (22)$$

where $\tilde{G}_+(z)$ indicates non-minimum phase characteristic of system. For ideal controller, (18) is transformed as:

$$y(z) = G_+(z)s(z) + \big(1 - G_+(z)\big)d(z) \quad (23)$$

Offset: $G_c(1) = 1/\tilde{G}(1)$ provides that the controller does not give any offset as given in (24).

$$\dot{x} = \big[A_1\big(D+\tilde{\delta}\big) + A_2\big(1-D-\tilde{\delta}\big)\big](X+\tilde{x}) + \big[B_1\big(D+\tilde{\delta}\big) + B_2\big(1-D-\tilde{\delta}\big)\big]\,(V_{in}+\tilde{v}_{in}) \quad (11)$$

$$V_{out}+\tilde{v}_{out} = \big[C_1\big(D+\tilde{\delta}\big) + C_2\big(1-D-\tilde{\delta}\big)\big](X+\tilde{x}) + \big[B_1\big(D+\tilde{\delta}\big) + B_2\big(1-D-\tilde{\delta}\big)\big](V_{in}+\tilde{v}_{in}) \quad (12)$$

$$\dot{x} = [A_1D + A_2D^-]X + [B_1D + B_2D^-]V_{in} + [(A_1 - A_2) + (B_1 - B_2)V_{in}]\tilde{\delta} \quad (13)$$

$$V_{out}+\tilde{v}_{out} = [C_1D + C_2D^-]X + [C_1D + C_2D^-]\tilde{x} + [(C_1 - C_2)X]\tilde{\delta} + \big[D_1\big(D+\tilde{\delta}\big) + D_2(D^- - \tilde{\delta})\big]V_{in} \quad (14)$$

$$X(s) = [sI - (A_1D + A_2D^-)]^{-1}[(A_1 - A_2)X + (B_1 - B_2)V_{in}]\tilde{\delta}(s) \quad (15)$$

$$\frac{V_{out}}{\tilde{\delta}}(s) = [D_1D + D_2D^-][sI - (A_1D + A_2D^-)]^{-1}[(A_1 - A_2)X + (B_1 - B_2)V_{in}] + [(C_1 - C_2)X] \quad (16)$$

$$\lim_{t\to\infty} y(t) = \frac{G(1)\,\tilde{G}(1)^{-1}}{1+\tilde{G}(1)^{-1}(G(1)-\tilde{G}(1))}(1 - d(1)) + d(1) = 1 \quad (24)$$

To provide that the system maintains robust against any distortion, low-pass filter is added to the controller as follows [12].

$$G_c(z) = \tilde{G}_-^{-1} F \quad (25)$$

$$F = diag\left(\frac{1-a_i}{1-a_i z^{-1}}\right); \quad 0 \le a_i \le 1 \quad (26)$$

Therefore, (18) is transformed as:

$$y(z) = G_+(z)\, F(z)\, (s(z) - d(z)) + d(z) \quad (27)$$

The filter design is expanded by [11] for the plant model given below:

$$F_r(s) = \frac{1}{(\lambda_r s+1)^n} \quad (28)$$

λ_r: Tuning parameter

n : Relative order of minimum phase

Distortion and variations can be evaluated against Integral Absolute Error (IAE) or Integral Square Error (ISE). IAE can be defined as the integral of absolute difference between reference and output signals and can be given as follows:

$$IAE = \int_0^{Ts} |s(t) - y(t)|\, dt \quad (29)$$

where T_s is settling time and the factorization can be minimized by IAE as (30):

$$G_+(s) = \prod_i (-\beta i s + 1) \quad Re(\beta i) > 0 \quad (30)$$

ISE is equivalent to the integral of the squared difference between the reference and output signals. This approach rapidly corrects errors while still allowing for minor errors to remain within an acceptable range.

$$ISE = \int_0^{Ts} (s(t) - y(t))^2\, dt \quad (31)$$

where *Ts* is settling time and the factorization can be minimized by ISE as (32):

$$G_+(s) = \prod_i \frac{-\beta i s+1}{\beta i s+1} \qquad Re(\beta i) > 0 \quad (32)$$

Consequently, the complementary sensitivity equations can be calculated as follows:

$$T_{IAE} = \prod_i (-\beta i s + 1)\, \frac{1}{(\lambda_r s+1)^n} \quad (33)$$

$$T_{ISE} = \prod_i \frac{-\beta i s+1}{\beta i s+1}\, \frac{1}{(\lambda_r s+1)^n} \quad (34)$$

4. DESIGN OF THE CONVERTER AND CONTROLLER (Dönüştürücü Ve Kontrolcü Tasarımı)

4.1. Calculation of the Inductor Value (İndüktör Değerinin Hesaplanması)

The L_1 and L_2 inductance values are calculated by minimum input voltage, which results a peak-to-peak ripple current of around 30% of maximum current. For inductors considered equal to each other, the ripple current is expressed as:

$$\Delta I_L = I_{in} * 30\% = \frac{I_{out} * V_{out}}{V_{in(min)}} * 30\% \quad (35)$$

Besides, the inductance is calculated as follows:

$$L_1 = L_2 = L = \frac{V_{in(min)}}{\Delta I_L * f_{sw}} D_{max} \quad (36)$$

4.2. Calculation of the Coupling Capacitor (C_1) (Kuplaj Kondansatörünün Hesaplanması)

The coupling capacitor's size is primarily determined by the RMS current, and the current flowing through the capacitor can be described as:

$$I_{C1_{rms}} = I_o * \sqrt{(V_o + V_D)/V_{in_{min}}} \quad (37)$$

Voltage ripple across coupling capacitor is defined peak-to-peak given below:

$$\Delta V_{C1} = \frac{I_o * D_{max}}{C_1 * f_{sw}} \quad (38)$$

4.3. Calculatıon of Output Capacıtor (C_2) (Çıkış Kondansatörünün Hesaplanması)

When the switching element is turned-on, the load-side current is supplied by output capacitor, and RMS current flowing through output capacitor can be given below:

$$I_{o_{rms}} = I_o * \sqrt{(V_{out} + V_D)/V_{in_{min}}} \quad (39)$$

Moreover, value of the output capacitor (C_2) can be expressed given below:

$$C_2 \ge \frac{I_o * D_{max}}{V_{ripple} * f_{sw}} \quad (40)$$

According to design parameters and specifications, calculated values are given in Table 1.

4.4. IMC Controller Design (IMC Kontrolcüsünün Tasarımı)

As a result of the design calculation, relation between small signal duty cycle and output is expressed as (41). The matrices of the zeros and poles can be defined as (42) and (43).

$$\frac{V_{out}}{\vec{\delta}}(s) = \frac{(1.441e-12)s^3 + (4.234e-07)s^2 + (0.0003408)s + 112.9}{(2.206e-17)s^4 + (2.793e-14)s^3 + (9.597e-09)s^2 + (7.541e-06)s + 0.9709} \quad (41)$$

$$Zeros = (1.0e+05)\begin{bmatrix} -2.9403 + 0.0000i \\ 0.0005 + 0.1633i \\ 0.0005 - 0.1633i \end{bmatrix} \quad (42)$$

$$Poles = (1.0e+04)\begin{bmatrix} -0.0027 + 1.6582i \\ -0.0027 - 1.6582i \\ -0.0606 + 1.2638i \\ -0.0606 - 1.2638i \end{bmatrix} \quad (43)$$

Table 1. Parameters and specifications of the SEPIC converter

Symbol	Description	Calculated
C_1	Coupling capacitor	≈ 135 µF
C_2	Output capacitor	≈ 271 µF
L_1	Inductor	≈ 9 µH
L_2	Inductor	≈ 9 µH
I_{L1}	Peak current of L_1 inductor	32.74 A
I_{L2}	Peak current of L_2 inductor	10.27 A
V_{RD1}	Reverse voltage of diode	64 V
$I_{Q1(max)}$	Maximum current of the switch	43.01 A
$I_{Q1_{rms}}$	RMS current of the switch	32.63

The reversible part of the equation according to the ISE criterion is:

$$G_+(s) = \frac{s^2-102s+2.665e08}{s^2+102s+2.665e08} \quad (44)$$

Also, the irreversible part is expressed as in (45). Elimination of unstable poles makes the controller as in (46). As a result, the filter is designed in the following manner:

$$F(s) = \frac{1e10}{0.012s^2+1.2s} \quad (47)$$

5. SIMULATION RESULTS (SİMÜLASYON SONUÇLARI)

In order to avoid overshoot in output voltage and to keep voltage fluctuations within the desired limits, simulation of the IMC method implemented to SEPIC topology is depicted in Figure 4. In addition, simulation studies are performed by using MATLAB/Simulink program.

Waveforms of output voltage, the zoom view of output voltage and output current at minimum input voltage and maximum duty cycle by using IMC method are illustrated in Figure 5, respectively.

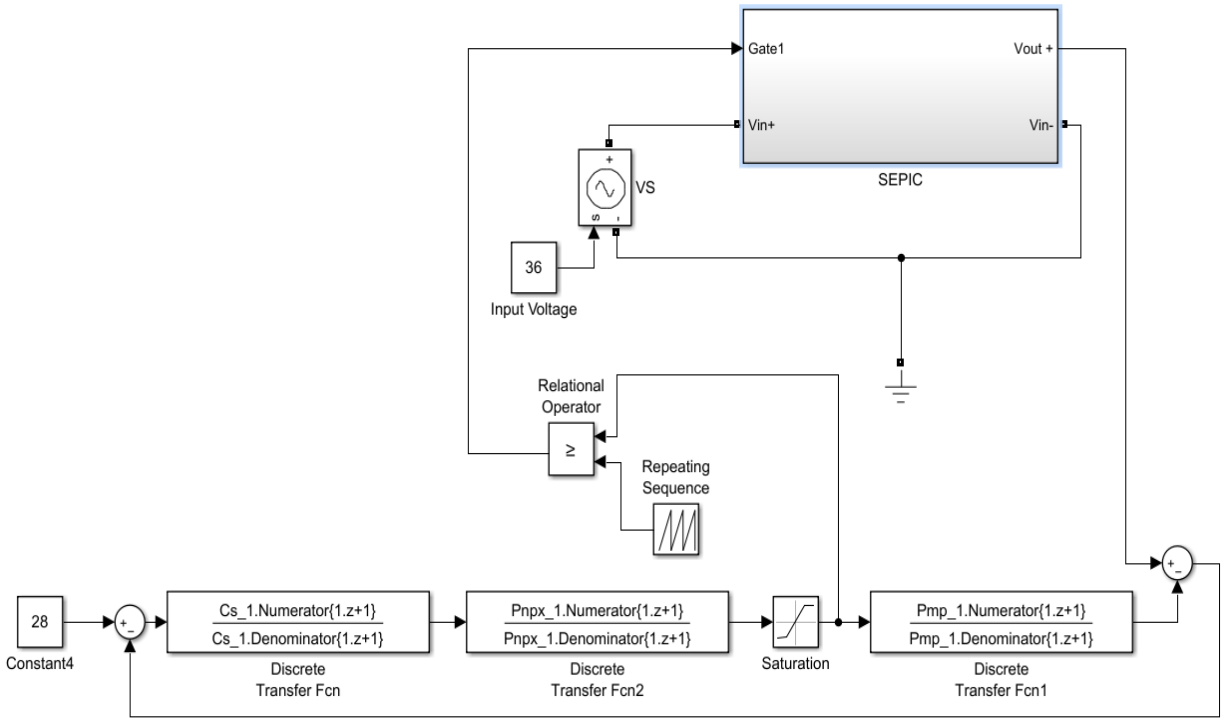

Figure 4. Simulation setup of the IMC method implemented to the SEPIC converter

$$G_-(s) = \frac{V_{out}}{\tilde{\delta}}(s) * \frac{1}{G_+(s)} = \frac{(6.531e04)s^3+(1.921e10)s^2+(1.937e13)s+5.118e18}{s^4+1266s^3+4.351e08s^2+3.419e11s+4.402e16} \quad (45)$$

$$C_s = \frac{1}{G_-(s)} * \frac{1}{(s-Poles(3,1))*(s-Poles(4,1))} = \frac{1.531e-05s^2+0.000833s+4210}{s^3+2.941e05s^2+2.965e08s+7.837e13} \quad (46)$$

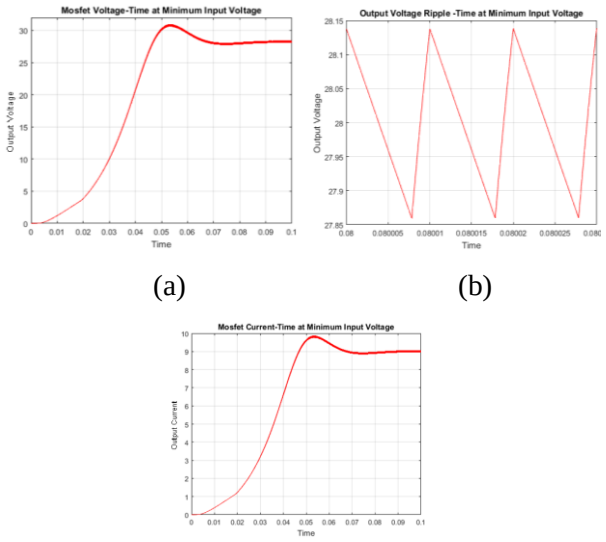

(a) (b)

(c)

Figure 5. a) Output voltage, b) zoom view of output voltage, c) output current

Waveforms of output voltage, the zoom view of output voltage and output current at maximum input voltage and minimum duty cycle by using IMC method are illustrated in Figure 6, respectively.

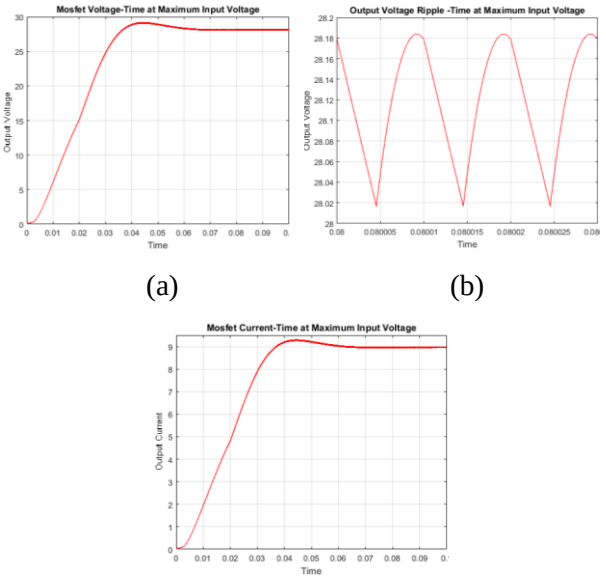

(a) (b)

(c)

Figure 6. a) Output voltage, b) zoom view of output voltage, c) output current

Figure 7 (a) depicts how the SEPIC converter reacts to changes in input voltage. Topology is controlled by the IMC method and input voltage is increased from 18 V to 30 V in 2 V steps. The results confirm that the transient response is fast and the steady-state error is minimal. The reply of the converter to the load variations has been performed at minimum input voltage by increasing the load by 30% every 100 ms. The response of output voltage and output current to load change is given in Figure 7 (b) and (c), respectively.

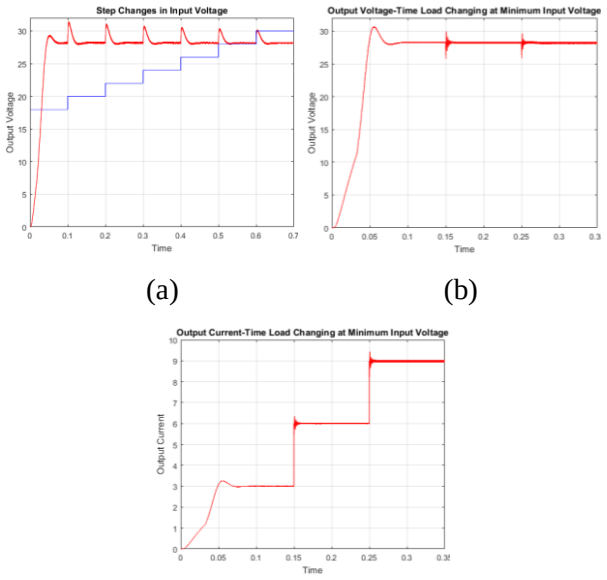

(a) (b)

(c)

Figure 7. (a) Response of the output voltage (red) and input voltage (blue) for input voltage variations (b) output voltage waveform during load variation (c) output current waveform during load variation

6. EXPERIMENTAL VERIFICATION (DENEYSEL DOĞRULAMA)

6.1. Design of SEPIC Converter (SEPIC Dönüştürücü Tasarımı)

The view of SEPIC power circuit designed to be used in experimental studies is given in Figure 8. Two layer PCB circuit is designed by using the Altium Designer program and consists of the following components: (1) Buck-Boost regulator circuit; (2) analog to digital converter (ADC) circuit; (3) SEPIC power circuit; (4) gate driver circuit; (5) Controller Board (STM32L100C-DISCO).

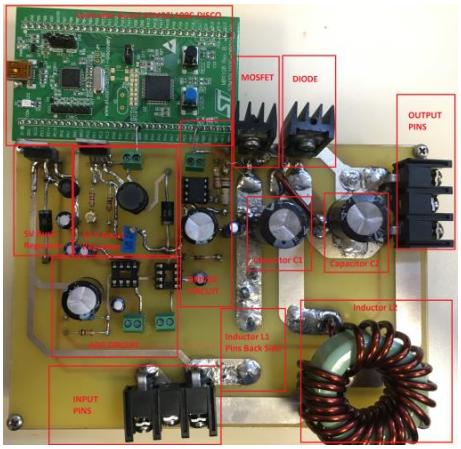

Figure 8. The laboratory setup of the SEPIC board

6.2. Test Results (Test Sonuçları)

This study examines the response of the SEPIC converter under different load conditions while in a steady-state. Therefore, input/output voltages, input/output currents, coupling capacitor voltage, V_{GS} and V_{DS} voltages of MOSFET are observed under the steady-state condition. All experimental data in this study is gathered using an oscilloscope and then translated into graphs using Microsoft Excel. Under the 10 Ω resistive load conditions and 32 V input voltage, Figure 9 (a) displays the waveforms of the input voltage, output voltage, and coupling capacitor voltage for the SEPIC converter. Besides, Figure 9 (b) shows the waveforms of the input and output currents of the SEPIC converter when subjected to 10 Ω resistive load and 32 V input voltage status.

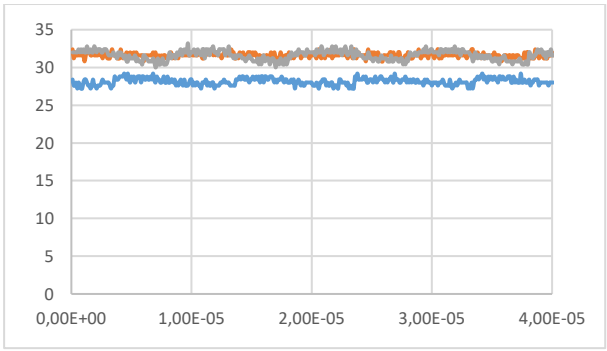

(a)

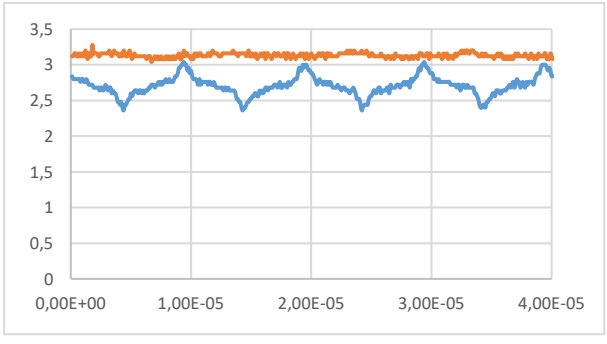

(b)

Figure 9. Waveforms under the 32 V input voltage and 10 Ω resistive load condition (a) input voltage (orange), output voltage (blue) and coupling capacitor voltage (grey) waveforms (b) input (orange) and output (blue) current waveforms

Under the 10 Ω resistive load and 32 V input voltage condition, Figure 10 (a) illustrates the voltage waveforms of the MOSFET V_{DS} and V_{GS} for the SEPIC converter. Besides, Figure 10 (b) displays the waveforms of the input/output and coupling capacitor voltages of the SEPIC converter when subjected to 10 Ω resistive load and 13 V input voltage conditions.

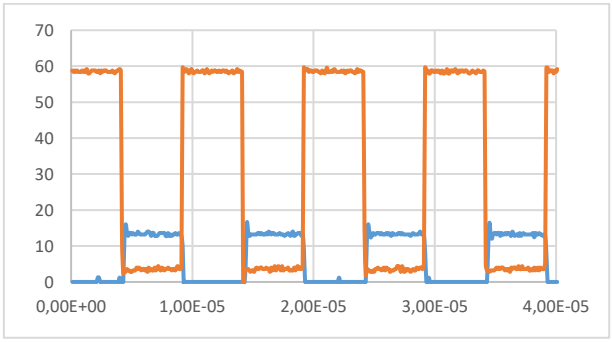

(a)

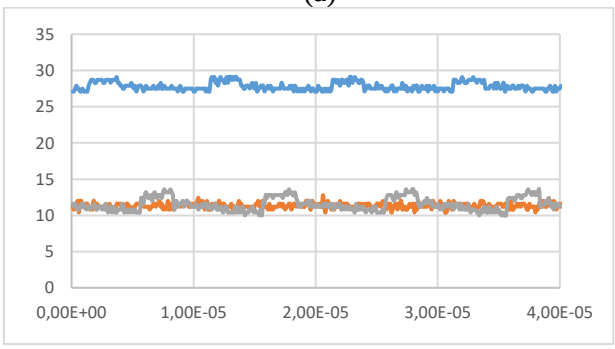

(b)

Figure10. (a) MOSFET V_{DS} (orange) and V_{GS} (blue) voltage waveforms under the 32 V input voltage and 10 Ω resistive load condition (b) input (orange)/output (blue) and coupling capacitor voltage (grey) waveforms under the 13 V input voltage and 10 Ω resistive load condition

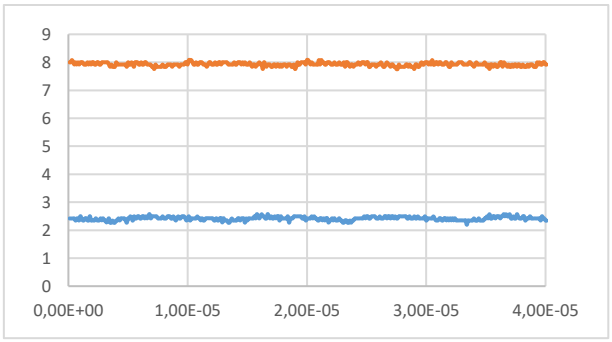

(a)

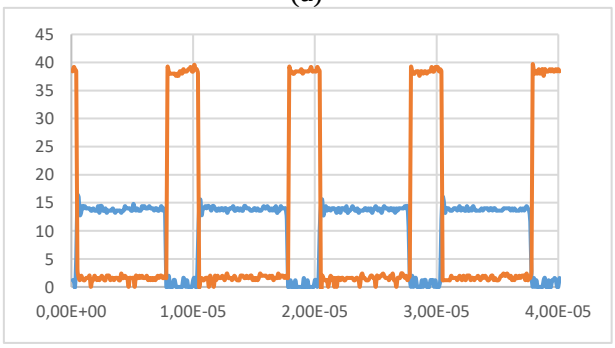

(b)

Figure 11. Waveforms under the 13 V input voltage and 10 Ω resistive load condition (a) input current (orange), output current (blue) waveforms (b) MOSFET V_{DS} (orange) and V_{GS} (blue) voltage

waveforms

Under the 10 Ω resistive load and 13 V input voltage condition, Figure 11 (a) illustrates the waveforms of the input/output currents of the SEPIC converter. In addition, Figure 11 (b) illustrates the voltage waveforms of MOSFET V_{DS} and V_{GS} for the SEPIC converter under the 10 Ω resistive load and 13 V input voltage conditions.

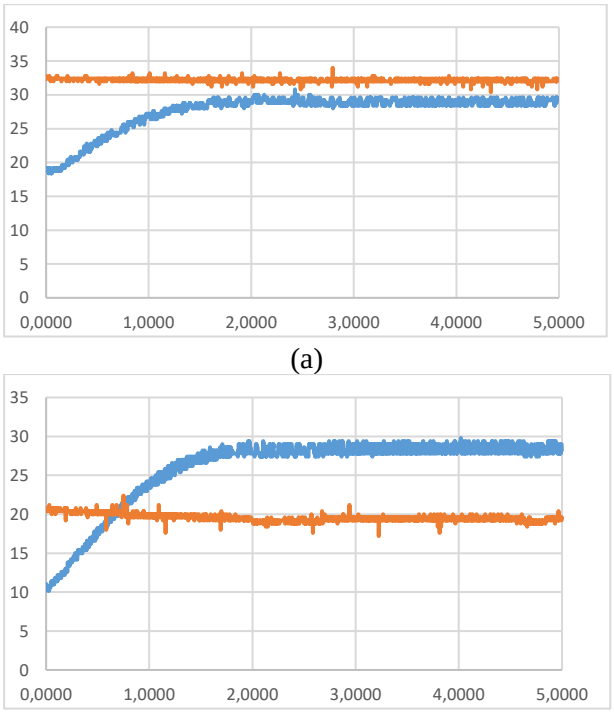

Fig. 12. (a) Input (orange)/output voltage (blue) waveforms under the 32 V input voltage and 10 Ω resistive load condition (b) input (orange)/output voltage (blue) waveforms under the 20 V input voltage and 10 Ω resistive load condition

This study has not only examined steady-state response of SEPIC converter under different load conditions but has also investigated its transient responses to variations in both load and input voltage. Under the 10 Ω resistive load and 32 V input voltage condition in the transient state, Figure 12 (a) illustrates the waveforms of input/output voltages of SEPIC converter. Also, Figure 12 (b) displays the waveforms of input/output voltages of SEPIC converter in transient state when subjected to the 10 Ω resistive load and 20 V input voltage conditions.

Output voltage overshoot ratios for proposed and conventional PI control methods in transient have been observed under different load and input voltage conditions and these data are presented in Table 2.

Under the transient state and load variation from 20Ω to 10Ω with 32 V input voltage, Figure 13 (a) illustrates the waveforms of input/output voltages of SEPIC converter. Besides, Figure 13 (b) shows the waveforms of input/output voltages of SEPIC converter under the transient state and load variation from 10Ω to 20Ω with 32 V input voltage.

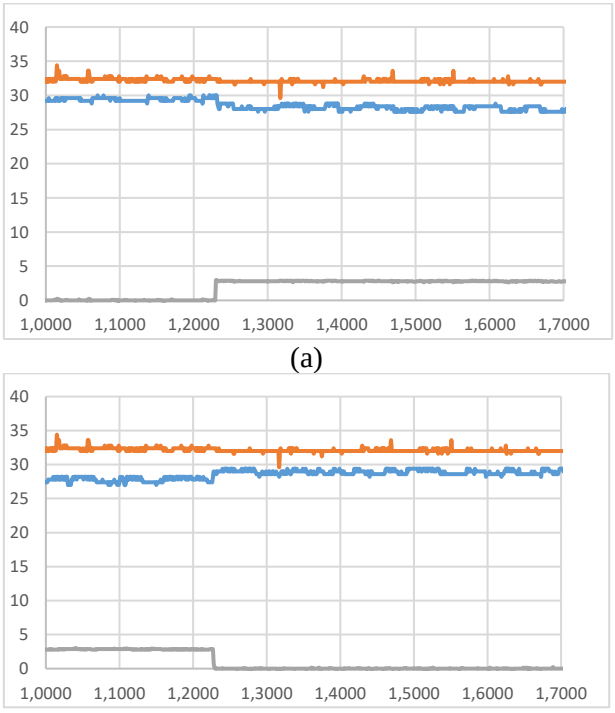

Figure 13. Input (orange)/output voltage (blue) waveforms under the 32V input voltage and resistive load variation (from 20Ω to 10Ω) (grey - step change) (b) input (orange)/output voltage (blue) waveforms under the 32V input voltage and resistive load variation (from 10Ω to 20Ω) (grey - step change)

Table 2. Voltage overshoot ratios for proposed and conventional PI control methods in transient state

	10 Ω		**15 Ω**			**20 Ω**		
Input voltage (V)	19.6V	32.15V	14.49V	19.99V	32.45V	10.41V	20.21V	32.49V
ICM Control Method								
Overshoot (%)	6.4%	10%	7.1%	8.6%	4.3%	8.6%	7.1%	5.7%
Conventional PI Control Method								

Overshoot (%)	7.3%	11.5%	7.9%	9.2%	4.8%	9.3%	7.8%	6.2%

Under the transient state and load variation from 20Ω to 15Ω with 15 V input voltage, Figure 14 (a) displays the waveforms of input/output voltages of SEPIC converter. In addition, Figure 14 (b) illustrates the waveforms of input/output voltages of SEPIC converter under transient state and load variation from 15Ω to 20Ω with 15 V input voltage.

Besides, output voltage overshoot ratios under different voltage and load variations for proposed and conventional PI control methods in transient state have been observed under different load and input voltage variations and these data that obtained from the experimental study are presented in Table 3.

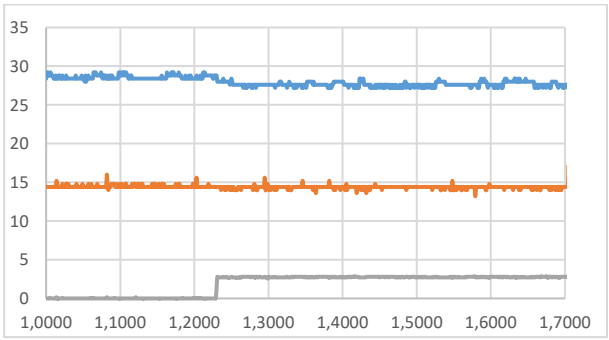

(a)

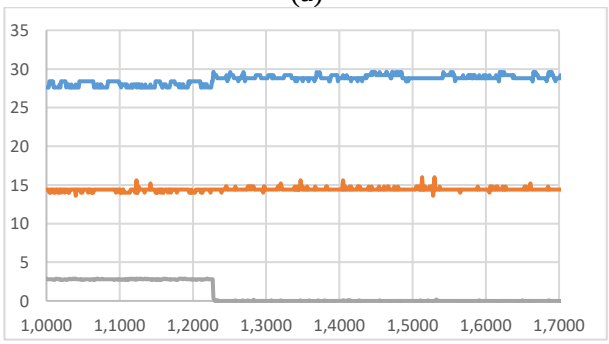

(b)

Figure 14. Input (orange)/output voltage (blue) waveforms under the 15 V input voltage and resistive load variation (from 20Ω to 15Ω) (grey - step change) (b) input (orange)/output voltage (blue) waveforms under the 15 V input voltage and resistive load variation (from 15Ω to 20Ω) (grey - step change)

7. CONCLUSION (SONUÇ)

The primary objective of this study is to design a controller that ensures the robust performance of the SEPIC converter, suitable for battery charging in military applications. To achieve this objective, an optimal internal model control (IMC) controller is developed to overcome improved setpoint tracking and minimal disturbance in SEPIC converter. Thus, problems faced in parameter setting of the PID controller, which is frequently used today, with the IMC controller have been compensated. The results obtained from the topology have been validated by simulation and experiments.

Simulation and experimental outcomes of SEPIC converter controlled by IMC technique revealed controller's robustness in both transient and steady-state conditions, when compared to the conventional PI method. Therefore, IMC can be regarded as a suitable control method for conventional power supplies that provide quick response and steady-state benefits.

DECLARATION OF ETHICAL STANDARDS (ETİK STANDARTLARIN BEYANI)

The author of this article declares that the materials and methods they use in their work do not require ethical committee approval and/or legal-specific permission.

AUTHORS' CONTRIBUTIONS (YAZARLARIN KATKILARI)

***Fatih Süleyman TAŞKINCAN*:** He conducted the literatüre review, experiments and analyzed the results.

***Ahmet KARAARSLAN*:** He conducted the conception, design and supervision process.

***Zafer ORTATEPE*:** He performed the interpretation, writing and critical review process.

CONFLICT OF INTEREST (ÇIKAR ÇATIŞMASI)

There is no conflict of interest in this stud

Table 3. Output voltage overshoot ratios under different voltage and load variations for proposed and conventional PI control methods in transient state

	10-20Ω	**20-10Ω**	**10-20Ω**	**20-10Ω**	**15-20Ω**	**20-15Ω**	**15-20Ω**	**20-15Ω**
Input voltage (V)	19.66V	32.15V	19.68V	32.18V	14.39V	14.40V	32.24V	32.30V

ICM Control Method								
Overshoot (%)	+8.57%	-8.57%	+5.7%	-4.3%	+4.3%	-2.86%	+2.86%	-2.86%
Conventional PI Control Method								
Overshoot (%)	+9.13%	-9.15%	+6.15%	-4.8%	+4.85%	-3.13%	+3.21%	-3.21%

REFERENCES (REFERANSLAR)

[1] Massey R.P., & Snyder E.C. (1977). High voltage single-ended DC/DC converter, IEEE Power Electronics Specialists Conference, 156-159.

[2] Luo F.L., & Ye H. (2004). Advanced DC/DC Converters, CRC Press, 55-60.

[3] Roberts S. (2016). DC/DC Book of Knowledge Practical tips for the User (3rd Ed.), 1-59.

[4] Font J., Vicuña L. G., Guinjoan F., Majó J., & Martinez L. (1987). A contribution to the analysis of the SEPIC converter, Proceedings of the IASTED Symposium Identification Modelling and Simulation, 355-358.

[5] Vicuña L. G., Guinjoan F., Majó J., &Martinez L. (1989). Discontinuous conduction mode in the SEPIC converter, MELECON '89: Mediterranean Electrotechnical Conference Proceedings. Integrating Research Industry and Education in Energy and Communication Engineering, 38-42.

[6] Eng V., Pinsopon U., & Bunlaksananusorn C. (2009). Modeling of a SEPIC converter operating in continuous conduction mode, 6th International Conference on Electrical Engineering/Electronics, Computer, Telecommunications and Information Technology, Pattaya, Chonburi, 136-139.

[7] Jose R., Anisha S., Vani V., & Kshemada D. (2015). DC-DC SEPIC converter topologies, International Journal of Research in Engineering and Technology, 04(05), 20-23.

[8] Bequette B. W. (1991). Nonlinear control of chemical processes: a review, Industrial &Engineering Chemistry Research, 1391-1413.

[9] Muhammad D., Ahmad Z., & Aziz N. (2010). Implementation of internal model control (IMC) in continuous distillation column, Proc. of the 5th International Symposium on Design, Operation and Control of Chemical Processes, 812-821.

[10] Garcia C. E., & Morari M. (1982). Internal model control. A unifying review and some new results, Industrial & Engineering Chemistry Process Design and Development, 21, 308-323.

[11] Morari M., & Zafiriou E. (1989). Robust Process Control, Prentice Hall.

[12] Garcia C. E., & Morari M. (1985). Internal model control 3. Multivariable Control Law Computation and Tuning Guidelines, Industrial & Engineering Chemistry Process Design and Development, 24, 484-494.

[13] Tarakanath K., Patwardhan S., & Agarwal V. (2014). Internal model control of dc-dc boost converter exhibiting non-minimum phase behavior, IEEE International Conference on Power Electronics, Drives and Energy Systems (PEDES), Bombay, India, 1-7.

[14] Sun X., Shi Z., Chen L., & Yang Z. (2016). Internal Model Control for a Bearingless Permanent Magnet Synchronous Motor Based on Inverse System Method, IEEE Transactions on Energy Conversion, 31(4), 1539-1548.

[15] Liu G., Chen L., Zhao W., Jiang Y., & Qu L. (2013). Internal Model Control of Permanent Magnet Synchronous Motor Using Support Vector Machine Generalized Inverse, IEEE Transactions Industrial Informatics, 9(2), 890-898.

[16] Rashid M. H. (2011). Power Electronics Handbook Devices, Circuit, and Applications (3rd Ed.), Elsevier.

[17] Middlebrook R., & Cuk S. (1976). A general unified approach to modelling switching converter power stages, IEEE Power Electronic Specialists Conference, 18-34.

[18] Polsky T., Horen Y., Bronshtein S., & Baimel D. (2018). Transient and Steady-State Analysis of a SEPIC Converter by an Average State Space Modelling, IEEE 18th International Power Electronics and Motion Control Conference (PEMC), Budapest, 211-215.